

Production of Hadrons with Large Transverse Momentum at 200 and 300 GeV*

J. W. Cronin, H. J. Frisch, and M. J. Shochet

The Enrico Fermi Institute, University of Chicago, Chicago, Illinois 60637

and

J. P. Boymond, P. A. Piroué, and R. L. Sumner

Department of Physics, Joseph Henry Laboratories, Princeton University, Princeton, New Jersey 08540

(Received 16 October 1973)

Differential cross sections as a function of transverse momentum are presented for the production at $\sim 90^\circ$ (in the c.m. system) of π^\pm , K^\pm , p , and \bar{p} in p -nucleus collisions at incident proton energies of 200 and 300 GeV.

Investigations of large-transverse-momentum (p_\perp) phenomena are interesting because of their possible relation to basic processes at small distances. Experimentally, it had been known¹ for some time that the p_\perp distributions of long-lived particles produced in high-energy hadron collisions were falling off exponentially (e^{-bp_\perp}), with the average transverse momentum $\langle p_\perp \rangle = 0.3-0.5$ GeV/c, independent both of the secondary-particle energy E and of the c.m. energy \sqrt{s} of the collision. Recent measurements² at the CERN intersecting storage rings (ISR) have in general confirmed these $\langle p_\perp \rangle$ values. However, at high p_\perp (>3 GeV/c), a much more copious pion production has been observed³⁻⁵ than predicted by the extrapolation of the data at small p_\perp (<1 GeV/c).

In an experiment at the National Accelerator Laboratory (NAL) we have measured, as a function of p_\perp , the invariant cross section $E d\sigma/d^3p$ for the production of π^\pm , K^\pm , p , and \bar{p} in p -nucleus collisions at incident proton energies of 200 and 300 GeV. The measurements were made in the region of 90° in the c.m. system of the incident proton and a single nucleon at rest.

Figure 1 shows a schematic view of the apparatus. The NAL proton beam, extracted from the

main ring and transported ~ 1.1 miles away to the target box of the proton east laboratory, impinged on a 2-in.-long, $\frac{1}{8}$ -in.-diam tungsten target. Particles emitted at 77 mrad ($\sim 90^\circ$ in the proton-nucleon c.m. system) relative to the direction of the incident proton beam traversed an ~ 330 -ft-long magnetic spectrometer consisting of a quadrupole doublet, two collimators, two bending magnets, and four scintillation hodoscopes H_1-H_4 . The momentum acceptance was 10% with a solid angle $\Delta\Omega = 17 \mu\text{sr}$. Each hodoscope consisted of a 4-in.-wide, 2-in.-high, $\frac{1}{4}$ -in.-thick trigger counter (A) followed by an array of five horizontal and seventeen vertical $\frac{1}{8}$ -in.-thick scintillator channels. This arrangement allowed us to determine the momentum of individual events to within $\pm 1\%$, and to reconstruct the position of each track at the target to within ± 0.4 in. horizontally and ± 0.08 in. vertically. This check was essential at high momentum to eliminate background.

Particles were identified in the Cherenkov counter located between H_3 and H_4 . It was an 80-ft-long, 1-ft-diam stainless-steel tube with nonreflecting walls, bolted to a 6-ft-long, 2-ft-diam optical section in which the Cherenkov light was split into two channels (0-9 and 9-38 mrad), and

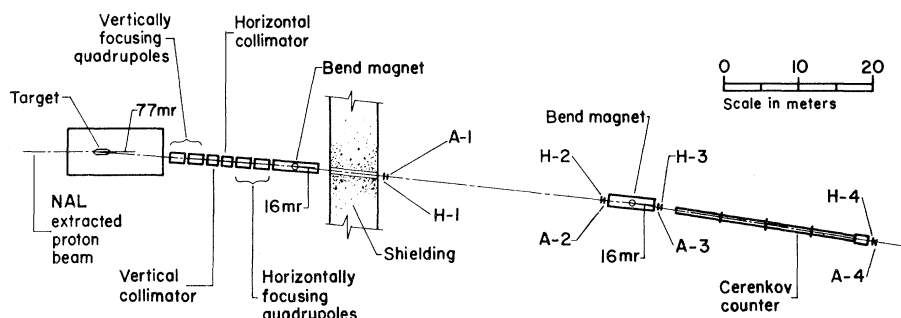


FIG. 1. Experimental arrangement.

TABLE I. Invariant cross section per nucleon (see text), $E d\sigma/d^3p$ ($\text{cm}^2 \text{GeV}^{-2}$), for π^\pm mesons produced at $\sim 90^\circ$ c.m. in p -W collisions, and particle ratios at 200 and 300 GeV incident proton energy. At each p_\perp value the top line refers to π^+ , K^+/π^+ , and \bar{p}/π^+ , respectively, and the bottom line to π^- , K^-/π^- , and \bar{p}/π^- . Errors on the cross sections do not include the uncertainty in the absolute calibration.

p_\perp (GeV/c)	200 GEV			300 GEV		
	$E d\sigma(\pi)/d^3p$	K/π	\bar{p}/π	$E d\sigma(\pi)/d^3p$	K/π	\bar{p}/π
0.76	$(2.69 \pm 0.13) \times 10^{-27}$ $(2.08 \pm 0.10) \times 10^{-27}$	0.33 ± 0.05 0.23 ± 0.03	0.37 ± 0.05 0.041 ± 0.003	$(2.89 \pm 0.14) \times 10^{-27}$ $(2.55 \pm 0.13) \times 10^{-27}$		
1.14	$(3.96 \pm 0.20) \times 10^{-28}$ $(3.21 \pm 0.16) \times 10^{-28}$	0.358 ± 0.029 0.165 ± 0.013	0.646 ± 0.007 0.104 ± 0.002	$(4.14 \pm 0.21) \times 10^{-28}$ $(4.12 \pm 0.20) \times 10^{-28}$		
1.53	$(6.04 \pm 0.30) \times 10^{-29}$ $(5.31 \pm 0.27) \times 10^{-29}$	0.331 ± 0.020 0.186 ± 0.011	0.824 ± 0.009 0.106 ± 0.002	$(6.26 \pm 0.31) \times 10^{-29}$ $(7.07 \pm 0.35) \times 10^{-29}$	0.343 ± 0.021 0.201 ± 0.012	0.647 ± 0.007 0.127 ± 0.002
2.29	$(2.56 \pm 0.13) \times 10^{-30}$ $(2.03 \pm 0.10) \times 10^{-30}$	0.434 ± 0.021 0.204 ± 0.010	1.020 ± 0.011 0.093 ± 0.003	$(2.95 \pm 0.15) \times 10^{-30}$ $(2.97 \pm 0.15) \times 10^{-30}$	0.421 ± 0.018 0.231 ± 0.010	0.871 ± 0.009 0.124 ± 0.002
3.05	$(1.25 \pm 0.06) \times 10^{-31}$ $(0.98 \pm 0.05) \times 10^{-31}$	0.485 ± 0.015 0.201 ± 0.006	1.093 ± 0.011 0.076 ± 0.001	$(1.77 \pm 0.09) \times 10^{-31}$ $(1.59 \pm 0.08) \times 10^{-31}$	0.514 ± 0.015 0.260 ± 0.008	0.871 ± 0.004 0.104 ± 0.001
3.81	$(6.77 \pm 0.34) \times 10^{-33}$ $(5.01 \pm 0.25) \times 10^{-33}$	0.522 ± 0.024 0.191 ± 0.007	1.07 ± 0.02 0.044 ± 0.003	$(1.35 \pm 0.07) \times 10^{-32}$ $(1.14 \pm 0.06) \times 10^{-32}$	0.532 ± 0.020 0.214 ± 0.008	0.816 ± 0.013 0.069 ± 0.003
4.58	$(3.86 \pm 0.19) \times 10^{-34}$ $(2.85 \pm 0.14) \times 10^{-34}$	0.536 ± 0.033 0.170 ± 0.014	1.11 ± 0.03 0.033 ± 0.003	$(8.78 \pm 0.42) \times 10^{-34}$ $(8.46 \pm 0.46) \times 10^{-34}$	0.531 ± 0.022 0.205 ± 0.008	0.742 ± 0.015 0.043 ± 0.002
5.34	$(2.38 \pm 0.12) \times 10^{-35}$ $(1.65 \pm 0.08) \times 10^{-35}$	0.64 ± 0.07 0.15 ± 0.03	1.09 ± 0.07 0.029 ± 0.014	$(9.45 \pm 0.57) \times 10^{-35}$ $(6.99 \pm 0.34) \times 10^{-35}$	0.50 ± 0.06 0.19 ± 0.02	0.67 ± 0.05 0.039 ± 0.007
6.10	$(1.30 \pm 0.19) \times 10^{-36}$ $(1.06 \pm 0.12) \times 10^{-36}$	0.55 ± 0.19 0.08 ± 0.07	0.98 ± 0.17 < 0.01	$(9.82 \pm 0.61) \times 10^{-36}$ $(7.42 \pm 0.53) \times 10^{-36}$	0.55 ± 0.08 0.16 ± 0.02	0.52 ± 0.05 0.023 ± 0.006
6.87	$(6.6 \pm 1.7) \times 10^{-38}$ $(5.2 \pm 1.6) \times 10^{-38}$					
7.25	$(1.6 \pm 0.9) \times 10^{-38}$					
7.63				$(6.9 \pm 2.0) \times 10^{-38}$ $(8.1 \pm 2.1) \times 10^{-38}$		

focused on 2-in. photomultipliers (RCA 3100 M). Depending on the momentum and the particle type the counter was filled either with He or CO_2 at pressures ranging from ~ 0 to 10 atm.

A charged particle was signaled by the coincidence $A_1 A_2 A_3 A_4$. Information from the counters was fed to a PDP-9 computer. The hodoscope information was used to reconstruct particle tracks through the spectrometer back to the target.

The proton beam striking the target was monitored by two three-counter telescopes located at 90° relative to the direction of the incident proton beam and directed at the target. The absolute calibration of the monitors against the proton beam intensity was done in two ways (radiochemical and ion chamber). However, while the relative accuracy of the monitors was better than 5%, their absolute calibration was estimated to be known only to $\sim 50\%$.

We measured the particle yields at laboratory momenta ranging from 10 to 100 GeV/c, corresponding to $p_\perp = 0.76$ to 7.6 GeV/c. In order to handle the high counting rates encountered below 40 GeV/c, smaller trigger counters were used and the hodoscopes removed. Accidental coincidences, monitored continuously, were found to be negligible except at high momenta (> 70 GeV/c) where the requirement that the ob-

served events originated in the target was essential in the elimination of this background. The data were corrected for nuclear absorption and multiple Coulomb scattering in the apparatus (significant only below 20 GeV/c), and, when appropriate, for particle decay.

The particle yields were converted into equivalent cross sections in p -nucleon collisions by using the following formula:

$$E \frac{d\sigma}{d^3P} = \frac{\sigma_p(\text{yield per incident proton})}{p^2(\Delta\Omega \Delta p/p)f},$$

where p denotes the lab momentum, σ_p the proton-nucleon total cross section which we took to be 40 mb, and f is the fraction of incident protons interacting in the target.⁶ Using an absorption cross section in W of 1635 mb, one obtains, for a 2-in. target, $f = 0.41$. The quantity $\Delta\Omega \Delta p/p = 1.7 \times 10^{-6}$, the spectrometer acceptance, was calculated by Monte Carlo techniques.

The production cross sections for π^\pm , and those for K^\pm , \bar{p} , and \bar{p} relative to pions of the same charge, are listed as a function of p_\perp in Table I. In Fig. 2 we have plotted, as an illustration, the π^- cross section against p_\perp at both incident proton energies. (The π^+ cross section has similar behavior.) We observe a falloff with p_\perp which is slower than exponential, and an energy depen-

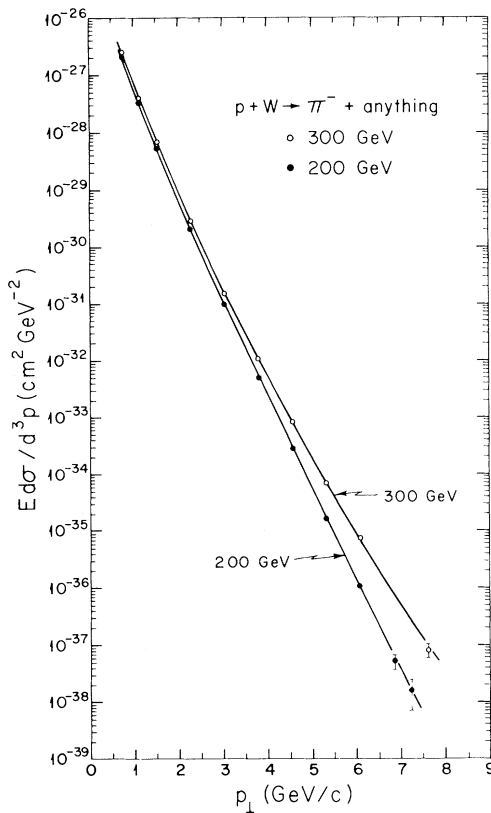


FIG. 2. Transverse-momentum distribution of π^- mesons produced at $\sim 90^\circ$ c.m. in p -W collisions at incident proton energies of 200 and 300 GeV.

dence which, though very small at low p_\perp , becomes stronger as p_\perp increases. This is in qualitative agreement with the work of the Saclay-Strasbourg group,³ and of the CERN-Columbia-Rockefeller group⁴ at the ISR.

Most of the theoretical models⁷ which have been proposed predict for the single-pion inclusive cross section at $\sim 90^\circ$ c.m. a behavior, at high p_\perp , of the form $g(s)f(x_\perp)$, where $g(s)$ is some function (generally a power law) of s , the square of the c.m. energy of the collision, and $f(x_\perp)$ is a function of the scaling variable $x_\perp = 2p_\perp/\sqrt{s}$. If our pion data can indeed be expressed in such a form, then the logarithm of the cross section plotted against x_\perp at both c.m. energies (19.4 and 23.8 GeV) should yield parallel curves, independent of the absolute calibration. Figure 3 shows that this is approximately so only at large x_\perp (> 0.4) where, for example, the form $s^{-5.4} \times \exp(-36x_\perp)$ is found to give a good representation of our data. At low x_\perp (< 0.3), however, the curves become slowly steeper as \sqrt{s} increases

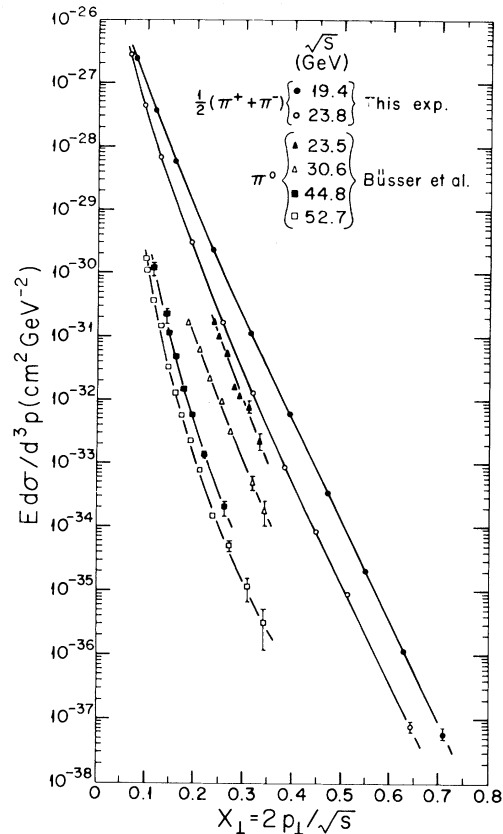


FIG. 3. The average of the π^+ and π^- invariant cross sections versus $x_\perp = 2p_\perp/\sqrt{s}$ at various c.m. energies. The data at $\sqrt{s} = 23.5, 30.6, 44.8,$ and 52.7 GeV are those of Ref. 4 and refer to π^0 . The discrepancy between the data at 23.8 and 23.5 GeV should not be considered significant.

(the higher-energy curves are the ISR π^0 data⁴).

The K^+ , p , and \bar{p} yields relative to pions are displayed as functions of x_\perp in Fig. 4. With the exception of p/π^+ the ratios do not change dramatically with incident proton energy. In fact, for $x_\perp > 0.4$ the ratios are, to a good approximation, independent of energy. For $p_\perp > 3.0$ GeV/c the ratios of heavy particles (K^+ , p , \bar{p}) to pions do not increase with p_\perp as suggested by measurements at the ISR at lower p_\perp .⁵ As x_\perp is increased from 0.2 to 0.5 the ratios K^+/K^+ and \bar{p}/p decrease by factors of ~ 2 and ~ 4 , respectively. This is a feature qualitatively similar to that found in had-ton production at small x_\perp and large $x = 2p_\parallel/\sqrt{s}$.

Finally it should be mentioned that auxiliary measurements made with beryllium and titanium targets established that none of the important features observed in tungsten were dependent on atomic number.

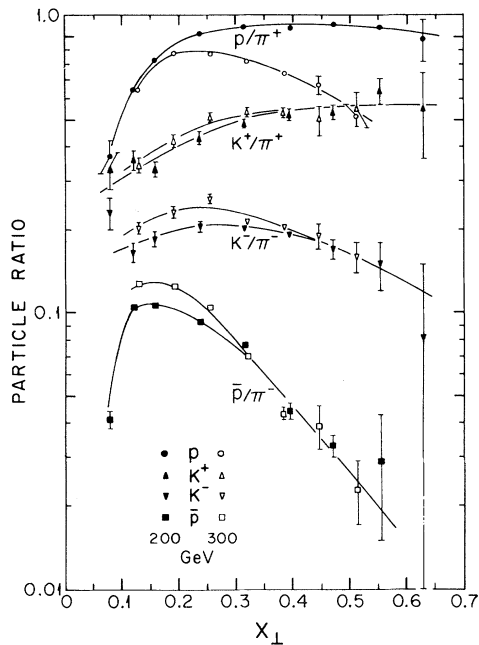


FIG. 4. Particle abundance relative to pions versus x_{\perp} .

We wish to express our appreciation to the staffs of NAL and especially of the proton area,

who have contributed enormous time and effort to make this experiment possible. We are also indebted to K. Wright for the excellent performance of the Cherenkov counter.

*Work supported by the National Science Foundation and the U.S. Atomic Energy Commission.

¹See, for example, G. Cocconi, *Nuovo Cimento* **57A**, 837 (1968).

²A. Bertin *et al.*, *Phys. Lett.* **42B**, 493 (1972); M. Banner *et al.*, *Phys. Lett.* **41B**, 547 (1972).

³M. Banner *et al.*, *Phys. Lett.* **44B**, 537 (1973).

⁴F. W. Büsser *et al.*, *Phys. Lett.* **46B**, 471 (1973).

⁵B. Alper *et al.*, *Phys. Lett.* **44B**, 521, 527 (1973).

⁶The diffractive scattering of a proton off the nucleus is not considered an interaction.

⁷See, for example, S. M. Berman, J. D. Bjorken, and J. B. Kogut, *Phys. Rev. D* **4**, 3388 (1971); R. Blankenbecler, S. J. Brodsky, and J. F. Gunion, *Phys. Lett.* **42B**, 461 (1972); P. V. Landshoff and J. C. Polkinghorne, *Phys. Lett.* **45B**, 361 (1973); S. D. Ellis and M. B. Kislinger, NAL Report No. PUB-73/40/THY (to be published).